JPEDAV (2005) 26:109-114
DOI: 10.1361/15477030523003
1547-7037/$19.00 ©ASM International

Phase Equilibria in the BaS-Ln_2S_3 Systems

O.V. Andreev, P.V. Miodushevscy, R. Serlenga, and N.N. Parsukov

(Submitted May 9, 2002; in revised form December 15, 2004)

A survey of available data for the BaS_2-Ln_2S_3 systems shows that the very light lanthanon systems form no intermediate phases but have extensive terminal solid solubilities of BaS in γ-Ln_2S_3 extending to near 50 mol.% BaS. For Ln = Nd and for all heavier lanthanons (smaller ionic radii, r_{Ln}^{3+}), an intermediate phase with stoichiometry of $BaLn_2S_4$ is formed. $BaLn_2S_4$ decomposes peritectoidally for Ln = Nd but melts congruently for Ln = Sm and for all heavier lanthanons. A second intermediate phase of stoichiometry, $Ba_3Ln_2S_6$, forms for Ln = Tb and for all heavier lanthanons (smaller ionic radii). For Ln = Lu, a third phase is formed at $BaLu_8S_{13}$. In all cases, $Ba_3Ln_2S_6$ melts peritectically, but $BaLu_8S_{13}$ melts congruently. The present article discusses: (1) three different techniques for synthesizing the intermediate phases; (2) the systems for Ln = Pr, Tb, and Y; and (3) a computer model for interpolating through the available data for the phase relationships in the nine systems that have been investigated to predict the phase diagrams for the seven systems for which there are limited or no data.

1. Introduction

In 1968, Flahaut and Laruelle[1] surveyed the available data for ternary combinations of the lanthanide elements with sulfur (S), selenium (Se), or tellurium (Te) plus a third element. In the 1990s, Andreev and coworkers[2-4] determined the pseudobinary phase diagrams of the Bas-Ln_2S_3 systems with Ln = lanthanum (La), neodymium (Nd), samarium (Sm), gadolinium (Gd), erbium (Er), and lutetium (Lu). In the course of the present investigation, the BaS-Ln_2S_3 systems with Ln = praseodymium (Pr), terbium (Tb), and yttrium (Y) were determinned to make a total of nine BaS-Ln_2S_3 systems with known phase equilibria. The present article presents (a) information on the preparation of the materials, (b) the methods for determining the phase diagrams, and (c) interpolation among the data for the known phase equilibria for the nine systems that have been investigated to predict the probable phase equilibria for the seven systems that have not yet been determined. Such prediction is a reasonable thing to do because other lanthanon series are known to exhibit systematic variations with progression from element to element.

2. Materials Preparation

2.1 General

Specimens for the study of phase equilibria in the BaS-Ln_2S_3 systems can be synthesized by three essentially different methods: (1), by passing a gaseous combination of H_2S and CS_2 through a bed of solid particles of oxides or salts; (2), by direct combination of the component sulfides; and (3), by direct reaction of the constituent elements. All methods involve mixtures of solid particles, so the kinetics of reaction involve temperature, particle size, thoroughness of mixing, and distribution of the Ba and Ln cations in the particles. The Ba-to-Ln ratio in the input mixture controls the stoichiometry of the product that is formed. All three methods produce massive specimens that are a transparent shade of brown. The specific shade depends upon composition.

2.2 Formation in a Mixed Bed of Particles

In the first method, specimens of various BaS-Ln_2S_3 intermediate compositions can be obtained by passing a flow of an H_2S-CS_2 gas mixture through a bed of mixed oxygen-containing substances (e.g., nitrates) with an appropriate Ba-to-Ln ratio. A schematic diagram of a typical apparatus for this process is shown in Fig. 1. An example of the sequence of phase changes that produce an intermediate phase composition is roughly:

$$\text{Input substances} \rightarrow {}^{1} \rightarrow BaS + Ln_2O_2S \rightarrow {}^{2} \rightarrow BaS + Ln_2S_3 \rightarrow {}^{3} \rightarrow BaLn_2S_4$$

The duration of stages 1 and 2 depends upon the kinetic factors previously noted, and the duration of stage 3 depends on those same factors and upon the intimacy of contact of Ba and Ln. If substances can be found wherein an appropriate ratio of Ba to Ln can occur in the same particle, the duration of stage 3 is reduced and the homogeneity of the product is enhanced. For example, a desirable situation can be achieved by producing oxides by the rapid thermal decomposition of jointly crystallized nitrates. Such a rapid decomposition can be achieved by rapidly heating a crucible (e.g., induction heating) to 1100 to 1200 K or, alternatively, by injecting the mixed nitrates into a furnace that is already at temperature. An alternative way of obtaining an appropriate sulfide mixture was developed. In this case, a mixture of jointly precipitated sulfates is treated with a stream of H_2 at 1150 to 1200 K and then is treated with a stream of mixed H_2S and CS_2 at 1300 to 1400 K.

2.3 Direct Combination of the Component Sulfides

For this approach, one must first obtain the component sulfides. Ln_2S_3 can be prepared by passing a gaseous mix-

O.V. Andreev, P.V. Miodushevscy, R. Serlenga, and **N.N. Parsukov,** Tyumen State University, Semakova Street 10, Tyumen 625003, Russia. Contact e-mail: koran@fromru.com.

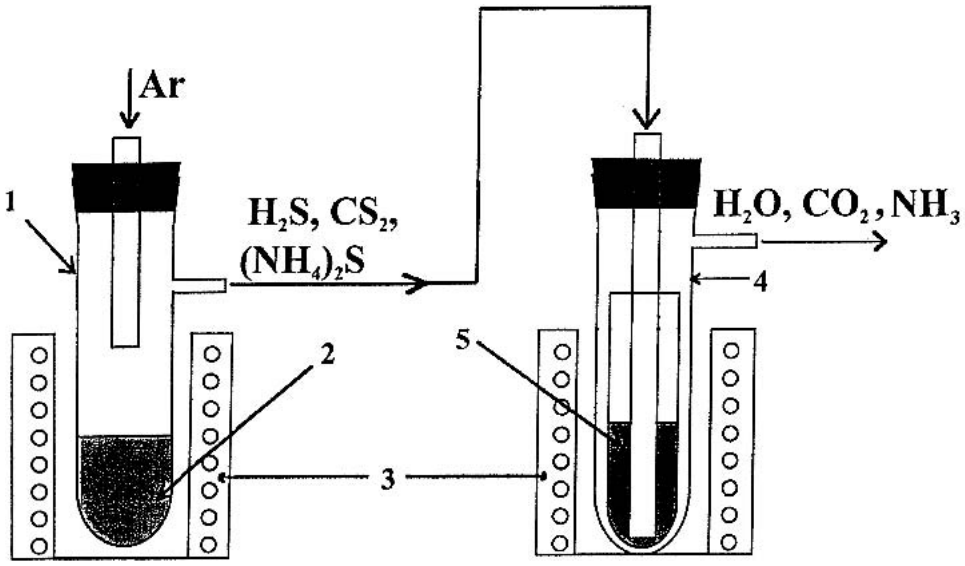

Fig. 1 Schematic diagram of an apparatus for preparing BaS-Ln_2S_3 material from a mixed bed of materials: 1, gas generating chamber; 2, NH_4CNS; 3, independently controlled resistance furnaces; 4, reaction chamber; 5, input charge of material

ture of H_2S and CS_2 through a bed of Ln_2O_3 or Ln halides at 1900 to 2400 K. This can be done in an apparatus such as that shown in Fig. 1. BaS can be produced by initially passing a stream of H_2 gas through a bed of BaO particles at temperatures in the range 1200 to 1270 K. Conversion of BaO to BaS is then completed by replacing the H_2 gas stream with a stream of H_2S. An appropriate apparatus would be similar to the reaction chamber seen in the right half of Fig. 1. The combination of BaS with Ln_2S_3 can be done under a protective atmosphere of S vapor to prevent thermal decomposition of the component and product sulfides. A schematic diagram for an appropriate apparatus for this combination is shown in Fig. 2. The S vapor is contained within a quartz envelop and is provided by a molten S reservoir. The well-mixed reactant sulfides were contained in an inert graphite crucible because the solid sulfides readily react with quartz. Reaction of the component sulfides was induced by heating to temperatures sufficiently high to produce S vapor pressures in the range 0.4 to 1.0 atm.

2.4 Synthesis from the Elements

Synthesis of phases from the constituent elements is the preferred method when oxygen impurities are to be kept to a minimum. In this case, the synthesis is done in evacuated quartz ampoules that are sealed, and the reactants are separated from the quartz in an inert container. Ba starts to interact with S even in the solid state. When transferring liquid S into the reaction chamber, the temperature remains constant until all Ba has been consumed. The lanthanons interact with S at temperatures of 750 to 1000 K. Because there is a tendency for the complex sulfides to decay at temperatures of 1100 to 1300 K, fusion and equilibration of a reacted mixture is done under an atmosphere of sulfur vapor. An apparatus such as that shown in Fig. 2 could be utilized.

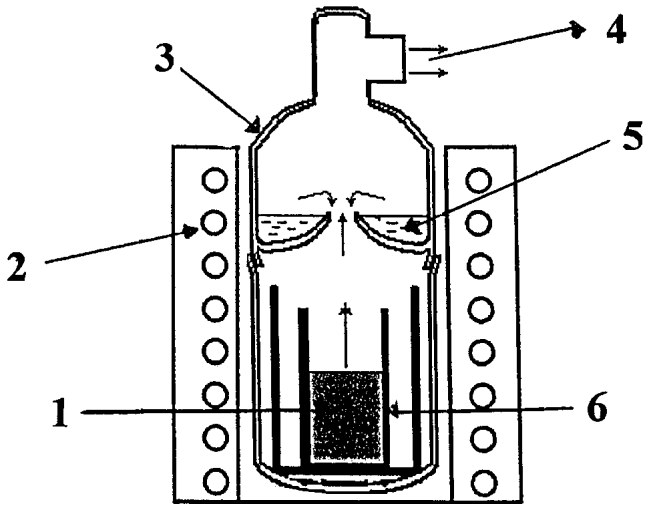

Fig. 2 Schematic diagram of an apparatus for preparing BaS-Ln_2S_3 from the sulfides, BaS and Ln_2S_3, or from the elemental metals, Ba and Ln: 1, input material; 2, resistance furnace; 3, reaction chamber; 4, evacuation port; 5, molten sulfur reservoir; 6, inert crucible

3. Determination of Phase Diagrams

The phase diagrams of the BaS-Pr_2S_3, BaS-Tb_2S_3, and BaS-Y_2S_3 systems were determined as a part of the present investigation. Though yttrium (Y) is not properly a lanthanon element, the Ln = Y diagram was included because the valence electron configuration of Y is the same as that of the lanthanons, and Y reacts in the same manner as the lanthanons. The behavior of Y is readily included with the lanthanon series by looking at the changing behavior as a function of the trivalent ionic radii rather than at the changing behavior as a function of atomic number. The BaS-Nd_2S_3,

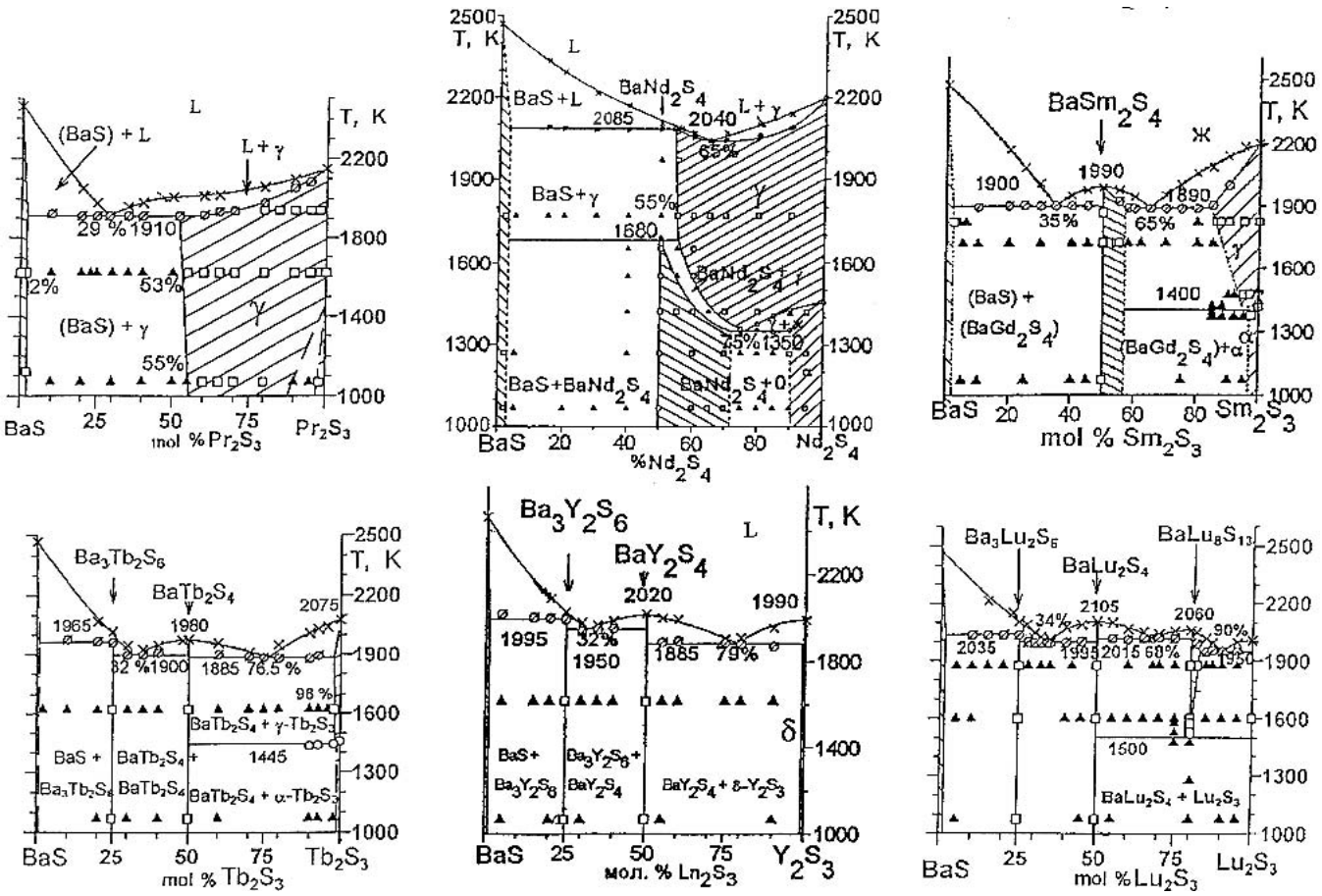

Fig. 3 Six of the nine BaS-Ln_2S_3 systems the phase equilibria of which have been experimentally determined

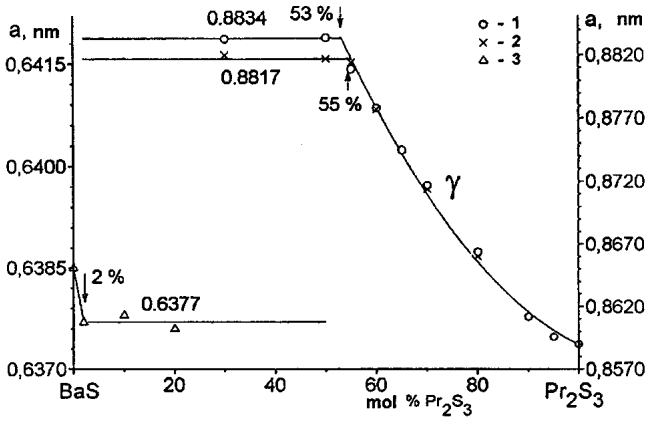

Fig. 4 Lattice parameters from x-ray diffraction of annealed and quenched samples of BaS-Pr_2S_3. 1 and 3, annealed at 1620 K; 2, annealed at 1070 K

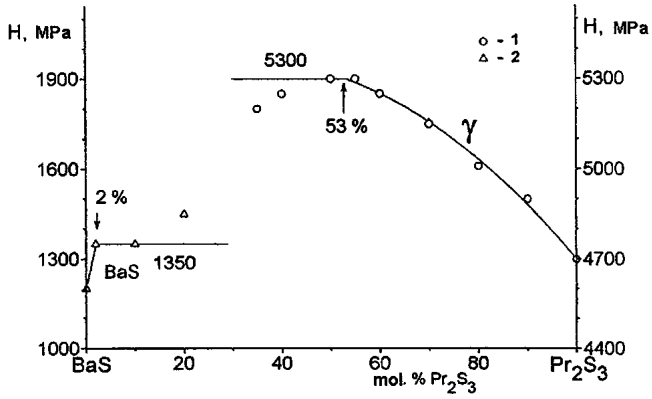

Fig. 5 Diamond pyramidal hardness data from samples of BaS-Pr_2S_3 annealed and quenched from 1620 K

BaS-Sm_2S_3, and BaS-Lu_2S_3 phase diagrams are shown together with BaS-Pr_2S_3, BaS-Tb_2S_3, and BaS-Y_2S_3 phase diagrams in Fig. 3. The reason for including these additional three diagrams is that, among the experimentally established phase diagrams, these six diagrams emphasize points of change. The BaS-Nd_2S_3 system is the first system in which any intermediate phase appears, and the phase is $BaNd_2S_4$. In this case, the phase decomposes peritectoidally, and it has a range of homogeneity. Inclusion of the BaS-Sm_2S_3 system in Fig. 3 shows that the $BaLn_2S_4$ phases increase in stability with decreasing trivalent atomic radius, and that $BaSm_2S_4$ melts congruently and with its range of homogeneity decreased with respect to that of $BaNd_2S_4$. The BaS-Tb_2S_3 system shows the first appearance of the second intermediate phase, $Ba_3Ln_2S_6$, and the BaS-Lu_2S_3 system

Table 1 Crystallographic data melting temperatures, and hardness values of various BaS–Ln_2S_3 phases

Ln in phase	Lattice parameters, nm			Unit cell, Vol/nm^3	T_m/K	DPH hardness, MPa	Density, kg/m^3
	a	*b*	*c*				
Ordered γ-terminal solid solutions at equimolar compositions space group *I*43*m*; *Pearson symbol cI*28; structure type Th_3P_4							
La	0.8909	…	…	0.7071	…	…	5.10
Ce	*0.8864*	…	…	*0.6964*	…	…	*5.21*
Pr	0.8829	…	…	0.6882	…	…	5.28
Nd (HT)	0.8793	…	…	0.6798	…	…	5.41
$BaLn_2S_4$ phases space group *Pnma*; Pearson symbol *oP*28; structure type $CaFe_2O_4$							
Nd (LT)	1.229	1.478	0.414	0.7520	1680	…	4.83
Sm	1.224	1.473	0.412	0.7428	1990	3000	4.98
Gd	1.221	1.465	0.408	0.7298	2000	3250	5.19
Tb	1.216	1.455	0.406	0.7183	2000	3300	5.32
Dy	*1.209*	*1.450*	*0.404*	*0.7082*	…	…	*5.48*
Ho	*1.207*	*1.447*	*0.402*	*0.7021*	…	…	*5.50*
Er	1.199	1.442	0.399	0.6899	2040	3450	5.85
Tm	*1.196*	*1.440*	*0.398*	*0.6855*	…	…	*5.75*
Yb	*1.191*	*1.433*	*0.396*	*0.6759*	…	…	*5.94*
Lu	1.190	1.432	0.396	0.6748	2105	3550	5.99
Y	1.216	1.456	0.406	0.7188	2020	3300	4.03
$Ba_3Ln_2S_6$ phases orthorhombic space group *Pmmn*; structure under investigation							
Tb	1.216	1.194	1.238	1.7975	1965	3240	…
Dy	*1.212*	*1.191*	*1.234*	*1.7813*	*1970*	…	…
Ho	*1.210*	*1.188*	*1.232*	*1.7710*	…	3030	…
Er	1.209	1.185	1.231	1.7636	2005	3200	…
Yb	*1.205*	*1.185*	*1.227*	*1.7251*	…	3030	…
Lu	1.204	1.183	1.228	1.7491	2035	2800	…
Y	1.212	1.19	1.233	1.7783	1995	2750	…

Note: Italicized data are interpolated values. HT, high temperature; LT, low temperature.

shows the appearance of a third intermediate phase, $BaLu_8S_{13}$.

The experimental techniques that have been used for determining all BaS-Ln_2S_3 phase diagrams are essentially the same. These include x-ray diffraction (XRD), metallography, hardness, differential thermal analysis (DTA), and visual polythermal analysis. This last technique is particularly powerful for determining the solidus and liquidus for transparent materials. Solidus points can be noted by observing the temperature at which sharp edges or corners initially soften and loose their sharpness. Liquidus points can be noted as the temperature at which the opalescence of a solid dispersed in a liquid changes to a clear transparent liquid. The solidus and liquidus points in Fig. 3 were determined by this technique with liquidus points being shown by Xs, and solidus points by Os. DTA was done with a W-Re thermocouple with ~3 g samples sealed under argon in quartz ampoules. Heating rates of 7 to 8 K/min were employed, and the DTA data were quite reproducible at temperatures below 1500 to 1600 K. At higher temperatures, the dissociation pressure of the sulfides created a problem and limited the accumulation of useful data to compositions near eutectic compositions. However, the technique was quite useful for determining eutectoid, peritectoid, and crystallographic phase transition temperatures, and the numerical values in Fig. 3 for those reactions are based on DTA measurements.

In the solid region, metallographic examination of quenched samples was used to determine whether a sample was single-phase or two-phase material. In Fig. 3, metallographic indications of two-phase regions are shown by ▲s, and single-phase regions are shown by □s. Phase boundaries were determined by XRD and by hardness measurements. Examples of such boundary determination for the BaS-Pr_2S_3 system are shown for the x-ray technique in Fig. 4, and for hardness measurements in Fig. 5. The x-ray lattice parameter data were taken with a DRON diffractometer (Bourevestnik Inc, St. Peterburg, Russia) with Ni-filtered CuKα radiation. The hardness testing was done by the diamond pyramidal load-indentation method with loads of 20 or 50 g. There is quite good agreement between the two techniques for the boundary compositions of both the BaS-rich terminal solid solution and the Pr_2S_3-rich terminal solid solution at 1620 K, which is the only temperature at which both techniques were applied. Because x-ray techniques can distinguish one phase from another in a two-phase region, x-ray measurements show a well-defined plateau in an equilibrated two-phase region. In contrast, the hardness data

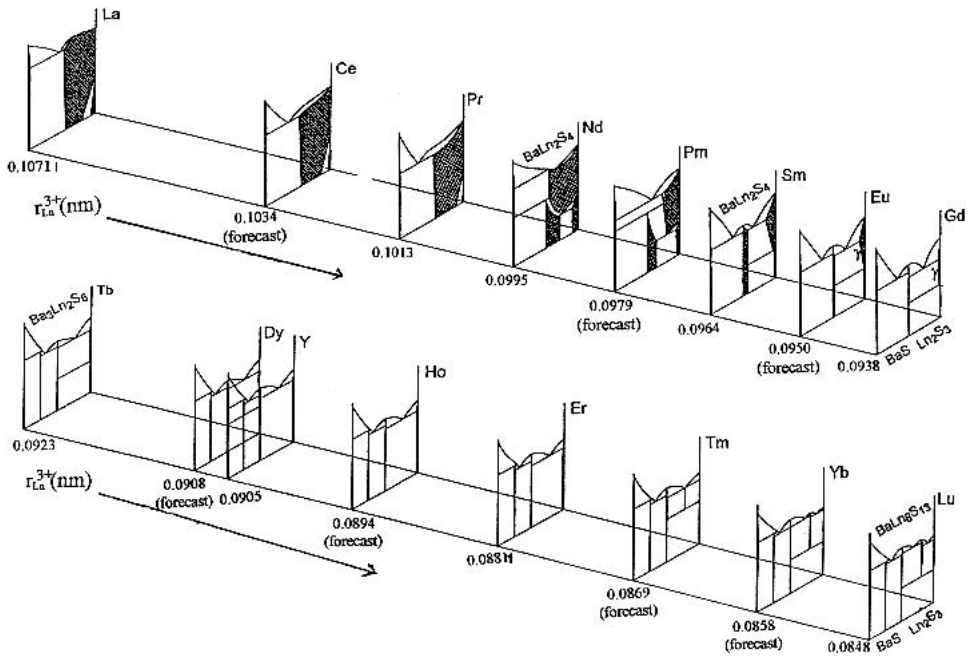

Fig. 6 Experimental and interpolated BaS-Ln_2S_3 phase diagrams plotted against trivalent ion core radii

show initial indications of a plateau in a two-phase region where one of the phases is predominant but tends to drift toward the hardness of the second phase as the second phase portion of a sample increases.

4. Interpolation

The available phase information from the nine BaS-Ln_2S_3 systems that have been determined shows that the phase diagrams with Ln = La or Pr are simple eutectic systems with no intermediate phases and with small terminal solid solubility of Ln_2S_3 in BaS but with extensive solid solubility of BaS in Ln_2S_3, reaching nearly 50 mol.% BaS in the high-temperature γ-Ln_2S_3 polymorph. For high BaS contents in the γ-Ln_2S_3-rich terminal solid solution, diffraction patterns show maxima characteristic of a Th_3P_4-type structure; this is indicative of ordering, with the larger Ba and Ln atoms preferentially occupying the Th sites and the smaller S atoms occupying the P sites. Data[5] for Th_3P_4 shows space group $I\bar{4}3$ and Pearson symbol *cI*28. The extent of the γ-Ln_2S_3-rich terminal solution decreases with decreasing trivalent ionic radius to approach a negligible extent at the Lu-end of the series. On the BaS-rich side of the diagram, the terminal solubility of Ln_2S_3 in BaS tends to be ~2 mol.% or less throughout the lanthanon series.

For Nd and for all heavier lanthanons with smaller trivalent ion radii, an intermediate phase occurs at a stoichiometry of $BaLn_2S_4$ ($BaS \cdot Ln_2S_3$). A single-crystal diffraction study as a part of the ongoing investigation of the BaS-Ln_2S_3 systems at this university has found all the $BaLn_2S_4$ phases to be isostructural with $CaFe_2O_4$, the structure[6] is orthorhombic, space group *Pnma,* Pearson symbol oP28. The range of homogeneity for $BaNd_2S_4$ extends from 50 to ~71 mol.% Nd_2S_3; for $BaSm_2S_4$ the range of homogeneity is reduced to 50 to ~57 mol.% Sm_2S_3, and the range decreases to an invariant stoichiometry at $BaGd_2S_4$ and continues to be invariant for the $BaLn_2S_4$ phase of all heavier lanthanons. It may also be noted that this phase in the BaS-Nd_2S_3 system decomposes peritectoidally but that for Ln = Sm and beyond the phases melt congruently. This appears to result from the increasing stability of the $BaLn_2S_4$ phases with attendant decreases in the range of homogeneity of the γ-Ln_2S_3 terminal solutions combining to cause the melting minimum of γ-Nd_2S_3 to become a eutectic reaction in the BaS-Sm_2S_3 system.

For Tb, Er, Y, and Lu, a second intermediate phase occurs in their diagrams at a stoichiometry of $Ba_3Ln_2S_6$ or ($3BaS \cdot Ln_2S_3$). The symmetry of these phases has been found to be orthorhombic with space group *Pmmn,* and the atomic loci are presently being investigated. It is believed to be likely these phases may represent a new structure type. Finally, in the Ln = Lu system, a third intermediate phase has been found at a stoichiometry of $BaLu_8S_{13}$ or ($BaS4Lu_2S_3$). This phase has a limited range of homogeneity. These indications of changing stabilities with decreasing radius of the trivalent ion of the lanthanons is consistent with the recent thermodynamic study by Khritohin et al.[7] The available lattice parameter data for the BaS-rich γ-Ln_2S_3 terminal solutions of La through Nd, the $BaLn_2S_4$ phases of Nd through Lu, and the phases of Tb through Lu are listed in Table 1 together with melting temperatures and hardness values; data for Y are included but those for Pm and Eu are omitted. In Table 1, values that were obtained by interpolation rather than by experiment are shown in italics.

A computer program was written to interpolate among all available phase diagram data to make estimations of the phase equilibria in the diagrams with Ln = cerium (Ce),

promethium (Pm), protactinium (Eu), dysprosium (Dy), holmium (Ho), thulium (Tm), and ytterbium (Yb). This program combined trends in compositional ranges of homogeneity, trends in temperatures of invariant reactions, trends in the temperatures and compositions of eutectic reactions, and the implications concerning phase stability from the study by Khritohin et al.[7] The results are plotted in Fig. 6. The scale of the diagram may cause some confusion, but the diagrams themselves all obey the phase rule for pseudobinary systems. For instance, it is not apparent in the BaS-La_2S_3 diagram that there is a liquidus-solidus two-phase field on the La_2S_3-rich side of the maximum melting temperature of γ-Ln_2S_3 phase, but such a two-phase field must be there. Also Fig. 6 appears to show the decomposition of the $BaTm_8S_{13}$ phase in the BaS-Tm_2S_3 diagram coinciding with the eutectic temperature to create a four-phase equilibrium. In actuality, the interpolated values are quite close, so the true situation may be that $BaTm_8S_{13}$ may decompose peritectoidally at a temperature very slightly below the eutectic temperature or it may decompose peritectically at a temperature very slightly above the eutectic temperature at a composition differing by a small amount on one side or the other from the eutectic composition.

5. Conclusion

From data for the phase equilibria in slightly over one half of the relevant BaS-Ln_2S_3 systems, phase equilibria for the remaining system have been inferred. Because the physical and chemical behavior of the lanthanons tend to vary systematically through the series, it is believed that the projected equilibria for the unmeasured systems have a high probability of reliability. One may rationalize the results in the following way. As one proceeds from La through Lu, the nuclear charge increases in increments of one. The lanthanide contraction occurs because the coulombic attractive force between the nucleus and an electron exceed the repulsive exchange and correlation forces from the increased number of 4f electrons. Thus, the ion core radii can be used as a qualitative gage to measure the net force field experienced by the valence electrons. In the present case, the increased field with lowered electronic energy states appears to stabilize the intermediate phase, in the order $BaLn_2S_4$, $Ba_3Tm_2S_6$, $BaTm_8S_{13}$, at the expense of the stability of the γ-Ln_2S_3 terminal solid solutions. In contrast, no significant change was observed in the terminal solubilities on the BaS side of the diagrams because the solubilities of Ln_2S_3 are all too small to make a significant contribution to stabilities.

References

1. J. Flahaut and P. Laruelle, Ternary Crystalline Combinations Formed by S, Se, or Te and a Rare Earth Element, *Progress in Science and Technology of Rare Earths,* Pergamon Press, Oxford, UK, Vol 3, 1968, p 149-208
2. O.V. Andreev, A.V. Kertman, and V.G. Bamburov, Interaction in Systems BaS-Ln_2S_3 (Ln = La, Nd), *Zh. Neorg. Khim.,* Vol 36, 1991, p 2623-2627 (in Russian)
3. O.V. Andreev, N.N. Parashykov, A.V. Kertman, and G.M. Kuzmicheva, *Zh. Neorg. Khim.,* Vol 43, 1998, p 679-683 (in Russian)
4. O.V. Andreev, N.N. Parshykov, and V.G. Bamburov, Phase Diagrams in Systems BaS-Ln_2S_3 (Ln = Sm, Gd), *Zh. Neorg Khim.,* Vol 43, 1998, p 853-857 (in Russian)
5. P. Villars and L.D. Calvert, *Pearson's Handbook of Crystallographic Data for Intermetallic Phases,* American Society for Metals, Vol 1, 1939, p 733, and Vol 3, 1939, p 2978
6. P. Villars and L.D. Calvert, *Pearson's Handbook of Crystallographic Data for Intermetallic Phases,* American Society for Metals, Vol 1, 1937, p 262, and Vol 2, 1937, p 1397
7. N.A. Khritohin, O.V. Andreev, O.Y. Mitroshin, and A.A. Korotkov, Thermodynamics of Phase Changes in Systems BaS-Ln_2S_3 (Ln = Pr, Sm, Gd, Tb, Er, Lu), *J. Phase Equilib. Diffus.,* Vol 25, 2004, p 515-519